Clinical Neurophysiology 139 (2022) 49–57

Contents lists available at ScienceDirect

Clinical Neurophysiology

journal homepage: www.elsevier.com/locate/clinph

Virtual implantation using conventional scalp EEG delineates seizure onset and predicts surgical outcome in children with epilepsy

Lorenzo Ricci [a], Margherita Matarrese [b,c,d], Jurriaan M. Peters [e], Eleonora Tamilia [f], Joseph R. Madsen [g], Phillip L. Pearl [e], Christos Papadelis [c,d,h,*]

[a] Unit of Neurology, Neurophysiology, Neurobiology, Department of Medicine, University Campus Bio-Medico of Rome, Rome, Italy
[b] Unit of Non-Linear Physics and Mathematical Modelling, Engineering Department, University Campus Bio-Medico of Rome, Rome, Italy
[c] Jane and John Justin Neurosciences Center, Cook Children's Health Care System, Fort Worth, TX, USA
[d] Department of Bioengineering, University of Texas at Arlington, Arlington, TX, USA
[e] Division of Epilepsy and Clinical Neurophysiology, Department of Neurology, Boston Children's Hospital, Harvard Medical School, Boston, MA, USA
[f] Division of Newborn Medicine, Department of Medicine, Boston Children's Hospital, Harvard Medical School, Boston, MA, USA
[g] Division of Epilepsy Surgery, Department of Neurosurgery, Boston Children's Hospital, Harvard Medical School, Boston, MA, USA
[h] School of Medicine, Texas Christian University, Fort Worth, TX, USA

ARTICLE INFO

Article history:
Accepted 8 April 2022
Available online 26 April 2022

Keywords:
Epilepsy surgery
Pediatric epilepsy
Electrical source imaging
Virtual sensors

HIGHLIGHTS

- Virtual sensors using low-density scalp EEG can non-invasively delineate the seizure onset zone.
- Virtual sensors can aid the intracranial EEG placement and improve the presurgical workup of children with epilepsy.
- Concordance of virtually-defined seizure onset zone with the intracranial EEG seizure onset zone can predict outcome in children with epilepsy.

ABSTRACT

Objective: Delineation of the seizure onset zone (SOZ) is required in children with drug resistant epilepsy (DRE) undergoing neurosurgery. Intracranial EEG (icEEG) serves as gold standard but has limitations. Here, we examine the utility of virtual implantation with electrical source imaging (ESI) on ictal scalp EEG for mapping the SOZ and predict surgical outcome.
Methods: We retrospectively analyzed EEG data from 35 children with DRE who underwent surgery and dichotomized into seizure-free (SF) and non-seizure-free (NSF). We estimated virtual sensors (VSs) at brain locations that matched icEEG implantation and compared ictal patterns at VSs vs icEEG. We calculated the agreement between VSs SOZ and clinically defined SOZ and built receiver operating characteristic (ROC) curves to test whether it predicted outcome.
Results: Twenty-one patients were SF after surgery. Moderate agreement between virtual and icEEG patterns was observed (kappa = 0.45, $p < 0.001$). Virtual SOZ agreement with clinically defined SOZ was higher in SF vs NSF patients (66.6% vs 41.6%, $p = 0.01$). Anatomical concordance of virtual SOZ with clinically defined SOZ predicted outcome (AUC = 0.73; 95% CI: 0.57–0.89; sensitivity = 66.7%; specificity = 78.6%; accuracy = 71.4%).
Conclusions: Virtual implantation on ictal scalp EEG can approximate the SOZ and predict outcome.
Significance: SOZ mapping with VSs may contribute to tailoring icEEG implantation and predict outcome.

Abbreviations: AUC, Area Under the Curve; CI, Confidence Interval; DRE, Drug-Resistant Epilepsy; ldEEG, Low-Density scalp EEG; CT, Computerized Tomography; dSPM, dynamical statistical parametric mapping; ESI, Electric Source Imaging; EZ, Epileptogenic Zone; icEEG, Intracranial EEG; icEEG-defined SOZ, Seizure Onset Zone defined after inspection of intracranial EEG (reference standard); hdEEG, High-Density scalp EEG; MEG, Magnetoencephalography; MRI, Magnetic Resonance Imaging; MSI, Magnetic Source Imaging; NSF, Non Seizure-Free; OR, Odds Ratio; SF, Seizure-Free; SOZ, Seizure Onset Zone; VSs, Virtual Sensors.

* Corresponding author at: Jane and John Justin Neurosciences Center, Cook Children's Health Care System, 1500 Cooper St., Fort Worth, TX 76104, USA.
E-mail address: christos.papadelis@cookchildrens.org (C. Papadelis).

https://doi.org/10.1016/j.clinph.2022.04.009
1388-2457/

1. Introduction

For children suffering from drug-resistant epilepsy (DRE), surgical treatment provides the highest opportunity to achieve seizure-freedom or a significant decrease in seizure frequency (Ryvlin et al., 2014). To grant the best possible surgical outcome, i.e. seizure-freedom, the epileptogenic zone (EZ, the cortical area that is necessary for the generation of clinical seizures) needs to be resected or disconnected (Lüders et al., 2006). Thus, a comprehensive presurgical evaluation, which relies on a multimodal approach, is crucial for accurately delineating the EZ margins. Yet, identifying the EZ is challenging and presurgical tests may not be sufficient to localize the seizure onset zone (SOZ; i.e. the cortical zone where seizures originate), the most reliable estimator of the EZ (Ryvlin et al., 2014). In these cases, patients are referred to an invasive exploration that consists of long-term intracranial electrodes implantation (intracranial EEG, icEEG) directly into or onto the brain. Nonetheless, icEEG is limited by its partial brain coverage and surgical complications are possible (Cossu et al., 2005). The implantation of icEEG electrodes needs to be tailored precisely to each patient since the risk of complications escalates with the increasing number of implanted electrodes (Mullin et al., 2016). Furthermore, icEEG may not succeed in revealing the SOZ in some cases, despite using all conventional non-invasive studies, such as video-EEG and MRI (Juárez-Martinez et al., 2018). Additional information from non-invasive techniques is required to improve the SOZ localization and optimize the implantation of icEEG electrodes. Such information would offer a significant benefit in the clinical management of children with DRE undergoing epilepsy surgery.

Electric and magnetic source imaging (ESI/MSI) are currently employed for the non-invasive delineation of the EZ. Yet, their use is more commonly applied to localize the irritative zone (i.e. the brain area that generates interictal spikes), which is relatively large, often overlaps with eloquent areas, and does not necessarily coincide with the SOZ (Lüders et al., 2006, Rosenow and Lüders, 2001). High-density EEG (hdEEG) and magnetoencephalography (MEG) are used for ESI/MSI since they have been shown to be precise in the non-invasive localization of the SOZ (Duez et al., 2019, Pellegrino et al., 2016, Plummer et al., 2019, Sohrabpour et al., 2020). Nevertheless, the clinical utility of MEG is limited by its high costs and short recording time, which hinders the probability of recording seizures. Similarly, hdEEG is hampered by the length of time required for setup and patient preparation as well as the time-consuming process to analyze and review the EEG signals (Chu, 2015). Conventional low-density scalp EEG (ldEEG) is low-cost and extensively accessible in almost all epilepsy centers. Its use for ESI has long been considered inaccurate for a precise tailoring and definition of the SOZ (Song et al., 2015). However, in recent years there has been a growing interest in the exploitation of ESI using ldEEG for the localization of the irritative zone (Russo et al., 2016, Tamilia et al., 2019) and for the delineation of the SOZ in adults (Beniczky et al., 2013, Foged et al., 2020, Sharma et al., 2018, Staljanssens et al., 2017) and children (Ricci et al., 2021).

By using advanced ESI/MSI analysis, virtual sensors (VSs) can be recreated at a-priori defined target brain sites to rise the signal-to-noise ratio in specific regions of interest (Hillebrand et al., 2005, Tamilia et al., 2021), facilitating the non-invasive identification of the irritative zone (Mohamed et al., 2013, Nissen et al., 2017) and SOZ (Juárez-Martinez et al., 2018). Nonetheless, it is still unknown whether a non-invasive implantation of VSs using ldEEG can be exploited for the identification of the SOZ. Such virtual implantation has the potential to enhance presurgical planning and improve outcomes of epilepsy surgery.

We propose a novel approach to localize the SOZ noninvasively using a virtual implantation and recorded ictal onset patterns with ldEEG. We hypothesize that the noninvasively localized SOZ (through the "implantation" of VSs) is concordant with the clinical-defined SOZ from the icEEG and predicts surgical outcome. We also hypothesize that the virtually reconstructed ldEEG ictal patterns and icEEG ictal patterns will have a high agreement (Di Giacomo et al., 2019). To test our hypotheses, we reconstructed VSs at locations that matched the icEEG implantation in children with DRE undergoing surgery, identified on VSs ictal patterns recorded with ldEEG (19 channels), and compared them with ictal patterns recorded with icEEG. We also estimated a *virtually-defined SOZ* and compared it with the standard reference provided by the *icEEG-defined SOZ*.

2. Material and methods

2.1. Patient cohort

The research team retrospectively reviewed data from children with an official diagnosis of DRE who underwent evaluation for surgery at the Epilepsy Center of Boston's Children Hospital (BCH) between April 2010 and February 2017. The study included patients who satisfied the following criteria: (i) underwent long-term monitoring with ldEEG and icEEG; (ii) had at least one seizure during both ldEEG and icEEG recordings; (iii) underwent post-implantation computerized tomography (CT) and pre-operative MRI; (iv) underwent surgical resection after icEEG monitoring; and (v) their two-year postsurgical follow-up was available from their medical record. The data have been previously used for other studies from our group (Ricci et al., 2021). The BCH Institutional Review Board approved this study (IRB-P00022114; PI: Papadelis) waiving the need for written informed consents (Ricci et al., 2021).

2.2. Acquisition of ldEEG and icEEG

All patients underwent long-term monitoring with ldEEG using the standard clinical setup with 19 electrodes according to the international 10/20 system, plus two additional fronto-temporal leads (FT9 and FT10). Data were recorded using the XLTEK EMU40 system (Natus Inc., USA). A sampling rate of 512 or 1,024 Hz was used for these recordings. Impedances were kept below 10 KΩ during the entire recording. Reference and ground electrodes were placed in frontocentral areas.

The icEEG data were recorded using the LTEK NeuroWorks (Natus Inc., USA) with a sampling rate ranging between 500 and 2,000 Hz. For the recordings, subdural grids and strips (2.3-mm exposure diameter, 10-mm distance; Ad-Tech., USA) and/or depth electrodes (10 linearly arranged contacts: 1.1-mm diameter, 3–5 mm inter-distance; Ad-Tech., USA) were used. The epilepsy team had decided the location as well as the number and type of electrodes aiming to monitor all possible epileptogenic areas based on patient's presurgical evaluation.

2.3. MRI acquisition and co-registration with EEG

Anatomical MRIs were obtained with magnetization-prepared rapid acquisition gradient-echo sequences using a high-resolution 3 T scanner before and after surgical resection. For ldEEG, we manually co-registered the electrode locations with the patient's MRI based on the MNI coordinates of the 10–20 system (Ricci et al., 2021). For icEEG, we determined the anatomical location of each electrode's contact by co-registering the post-implantation CT with the preoperative MRI using *Brainstorm*

(Tadel et al., 2011). On the co-registered CT-MRI image, we determined each contact's coordinate by reviewing sagittal, coronal, and axial planes, and mapped on patient's 3D cortical surface reconstructed from the preoperative MRI using *FreeSurfer* (Dale et al., 1999, Ricci et al., 2021).

2.4. Identification of seizure onset

The ldEEG and icEEG data were reviewed for electro-clinical seizures by two experienced neurophysiologists blind to the clinical data (L.R. and J.M.P.). We defined the seizure onset as "a sudden change of activity that is distinct from the preceding background, followed by an evolution of this activity in both frequency and amplitude" (Verma and Radtke, 2006). Ictal onsets were identified and marked by L.R. and J.M.P. (who were blinded to each other's marking). We pre-processed the EEG data in *Brainstorm* (Tadel et al., 2011). We initially removed the DC offset and then applied a 60-Hz notch filter and a bandpass filter between 1 and 70 Hz. By using Independent Component Analysis, we removed components that corresponded to heart and eye-blinking activity (Nemtsas et al., 2017, Ricci et al., 2021).

2.5. VSs reconstruction

We reconstructed VSs in corresponding icEEG location in order to compare the proposed noninvasive methodology with the invasive gold standard (Fig. 1a&b). VSs were reconstructed for each ldEEG recorded seizures separately. In case where several stereotyped seizures were recorded in a patient, we analyzed only the seizure that was least affected by artifacts (Beniczky et al., 2013). In case where different seizures in the same patient were considered having different semiology or displaying distinct EEG patterns at onset, we analyzed each seizure separately (Beniczky et al., 2013).

2.6. ESI

We extracted cortical surfaces from the preoperative MRIs via *FreeSurfer* (Dale et al., 1999) and constructed realistic head models using OpenMEEG (Gramfort et al., 2010) (3-layer boundary elementary model) (Tamilia et al., 2019, Tamilia et al., 2021). Source space included the entire brain volume. We performed ESI on ldEEG recorded seizures blind to the patient's clinical history. The analysis was carried out using a time window around the seizure onset. We used dynamical statistical parametric mapping (dSPM) (Dale et al., 2000), a distributed source-modeling technique implemented in *Brainstorm*, to estimate brain activity within the source space. DSPM output was used to reconstruct the activity of selected brain regions (at the VSs locations), where the icEEG electrodes had been implanted during the patient's long-term monitoring. For each icEEG electrode (Fig. 1a), we defined nonoverlapping regions of interest (ROIs) that included the closest volume points around the electrode's center, up to 5 mm for stereo-EEG or up to 10 mm for subdural electrodes (Tamilia et al., 2021). Finally, we reconstructed VSs time series by computing its mean activation (mean across volume points) (Fig. 1c). ESI was performed retrospectively; thus, the ESI findings reported here did not influence the surgical decision.

2.7. Intracranial EEG-defined SOZ and virtually-defined SOZ

The *icEEG-defined SOZ* (Fig. 1d) was prospectively defined during the icEEG monitoring by pediatric neurologists based on the SOZ electrode/s displaying the earliest modification from the background activity coupled with each recorded seizure, independently

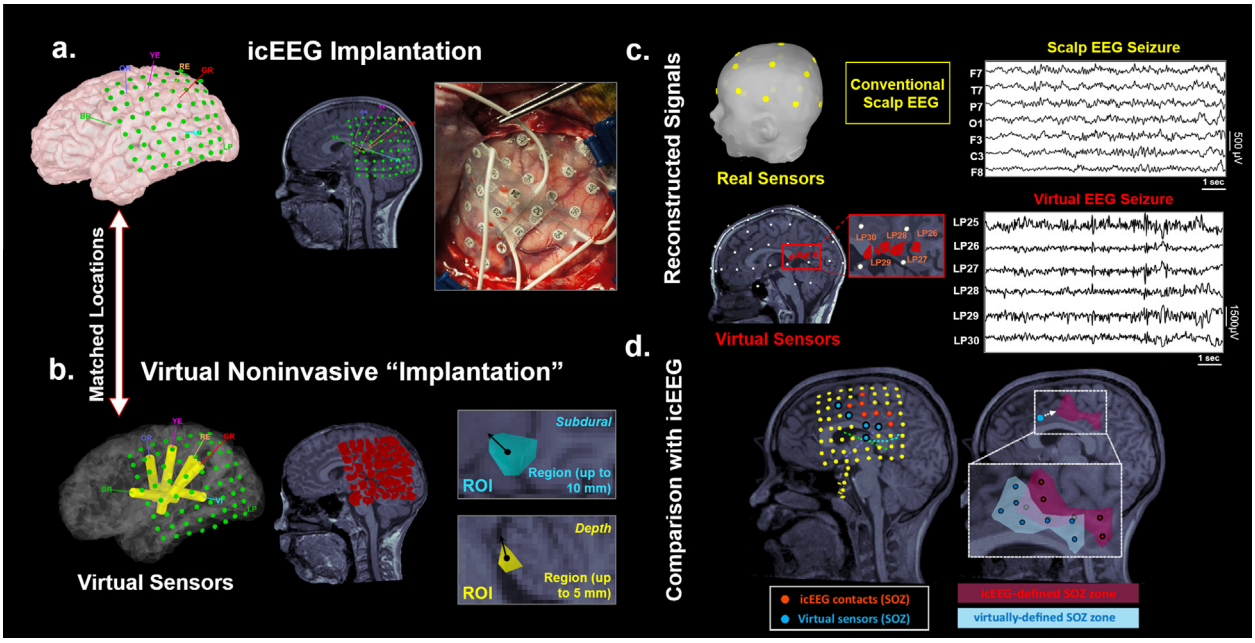

Fig. 1. Virtual Sensors (VSs) utilizing low-density scalp EEG (ldEEG). a. Intracranial EEG (icEEG) implantation of a 10-year-old boy with DRE and intracranial exploration of left parietal region and perisylvian area and placement of virtual sensors (VSs) based on the coordinates of icEEG electrodes (matched sites). **b**. Placement of VSs based on the icEEG electrodes coordinates (matched sites). Non-overlapping regions of interest (ROIs) were characterized for each contact in the patient's source space as described in Tamilia et al. (2021). **c**. Reconstruction of virtual EEG signal (time series): mean activity of conventional scalp electrodes (virtual signal) across time, reconstructed based on scalp EEG recorded seizure. **d**. Left: Localization of intracranial EEG (icEEG) electrodes on a patient's preoperative MRI after co-registration with post-implantation CT. Intracranial EEG electrodes that displayed the earliest ictal activation (*icEEG-defined seizure onset zone [SOZ]*) are marked in red. VSs that displayed the earliest ictal activation (*virtually-defined SOZ*) are marked in light blue. Right: The brain volume containing the icEEG-SOZ electrodes identifies the invasive reference standard (*icEEG-defined SOZ, red volume*). Similarly, brain tissue surrounding the VSs-SOZ defines the anatomical landmarks of the *virtually-defined SOZ (light blue volume)*.

from this study. For each patient, we defined the *icEEG-defined SOZ* site as the coordinates of all SOZ electrode/s (Alhilani et al., 2020, Ricci et al., 2021).

The *virtually-defined SOZ* (Fig. 1d) was retrospectively determined by visual inspection of ldEEG seizures reconstructed using VSs, and defined as the VSs showing the earliest change from the background activity coupled with each recorded seizure. The visual inspection of ictal onset patterns on VSs and definition of SOZ electrodes was performed by an experienced neurophysiologist (L.R.) blind to clinical information and post-surgical outcome.

2.8. Classification of ictal patterns and postsurgical outcome

We categorized each ictal pattern reconstructed with VSs as: (i) *low-voltage fast activity*: rhythmic activity that is clearly visible with frequencies more than 13 Hz; (ii) *rhythmic activity at ≤13 Hz:* sharply contoured rhythmic activity (most commonly in the alpha-theta range) with low- to medium-voltage amplitude; and (iii) *spike-and-wave activity*: spike-and-wave complexes (at a frequency of 2–4 Hz) with medium-to high-voltage amplitude (Perucca et al., 2013) (Fig. 2). Intracranial EEG seizures recorded during subsequent long-term monitoring registrations were also visually inspected and classified according to ictal patterns previously described. We determined the patients postsurgical outcome based on their most recent follow-up visit using the Engel scale (Engel Jr et al., 1993). We then dichotomized the patients into seizure-free (SF, Engel 1) and non-seizure-free (NSF, Engel ≥2).

2.9. Comparison of VSs with icEEG

We assessed the ability of VSs to localize the SOZ by comparing the *virtually-defined SOZ* (i.e., VSs where ictal onset patterns were identified) with the reference standard provided by the *icEEG-defined SOZ* (i.e., icEEG electrodes where ictal onset patterns were identified). We quantified the agreement (in percentage) between the *virtually-defined SOZ* and the *icEEG-defined SOZ*. We also assessed the anatomical concordance of the *virtually-defined SOZ* and the *icEEG-defined SOZ* at the sublobar level (Fig. 3). We identified 20 sublobar regions (Agirre-Arrizubieta et al., 2009, Ricci et al., 2021). If the reference standard's (*icEEG-defined SOZ*) sublobar regions matched the *virtually-defined SOZ*, this was considered concordant with the reference standard. If these localizations only partially matched the reference standard or were in different sublobar regions, the *virtually-defined SOZ* was considered discordant.

Further details about the anatomical landmarks of sublobar regions are provided in Fig. 4A.

2.10. Comparison between superficial and deep onset regions

To estimate whether the location of the SOZ (i.e., superficial vs. deep onset) may influence the ability of VSs to pinpoint the SOZ site, we compared the percentage agreement between the *virtually-defined SOZ* and the *icEEG-defined SOZ* among patients with superficial SOZ and deep SOZ. We considered as superficial seizure onset regions the following: (i) the superior; (ii) middle; and (iii) inferior frontal gyrus; (iv) the orbitofrontal region; (v) the lateral temporal region; (vi) the central region; (vii) the superior and (viii) inferior parietal lobules; (ix) the supramarginal and angular gyri; (x) the parieto-occipital region; and (xi) the occipital convexity (see Fig. 4A). We considered as deep seizure onset regions the following: (i) the opercular-insular region; (ii) the mesial part of the frontal, (iii) parietal, (iv) central and (v) occipital lobes; (vi) the mesial temporal lobe (including the amygdala, hippocampus, and para-hippocampal gyrus); (vii) the lingual gyrus; and the anterior (viii) and posterior (ix) part of the cingulate gyrus (see Fig. 4A).

2.11. Prognostic value for surgical outcome

To estimate the clinical value of virtual implantation for predicting the surgical outcome, we built receiver operating characteristic (ROC) curves on the percentage agreement and anatomical concordance of the *virtually-defined SOZ* with the reference standard. Seizure freedom following resection was considered to be the *ground truth*, i.e. unequivocal confirmation of EZ resection. We considered as: (i) true positives (TP), SF patients with high concordance between the *virtually-defined SOZ* and the reference standard; (ii) true negatives (TN), NSF patients with low concordance between the *virtually-defined SOZ* and the reference standard; (iii) false positives (FP), NSF patients with high

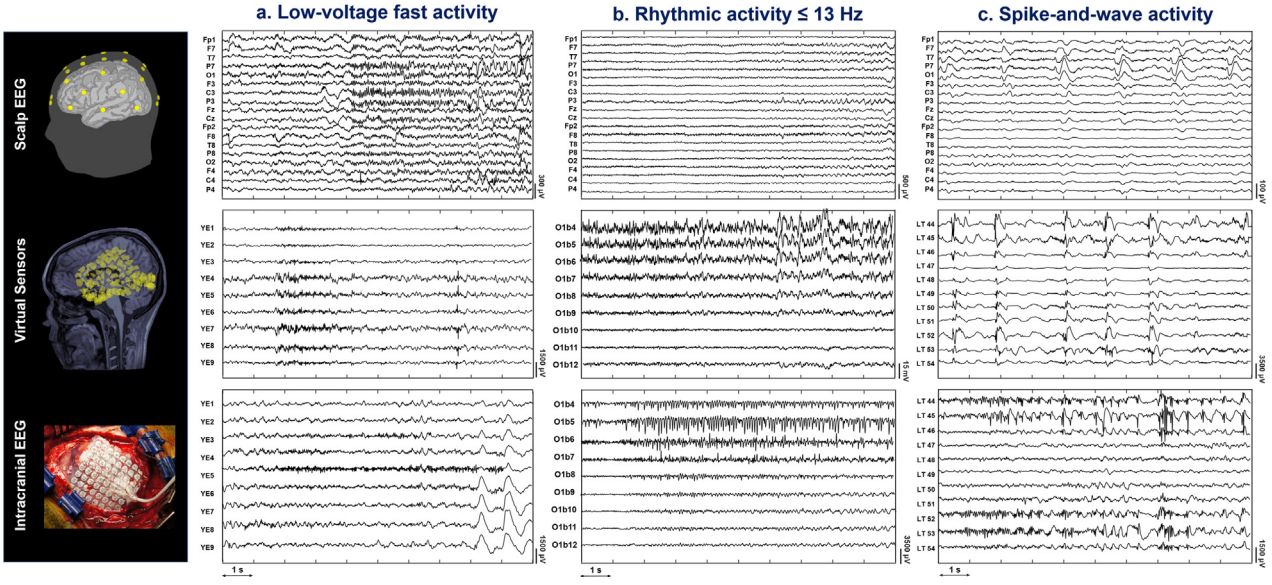

Fig. 2. Ictal electrographic patterns: comparison between virtual sensors and intracranial EEG. Reconstruction of ictal EEG signal using low-density scalp EEG (upper) and virtual sensors (VSs, middle) at matched intracranial EEG locations (lower). Ictal events were classified according to specific electrographic patterns: **a**. Low-voltage fast activity; **b**. Sharp rhythmic activity at ≤13H; or **c**. Spike-and-wave activity.

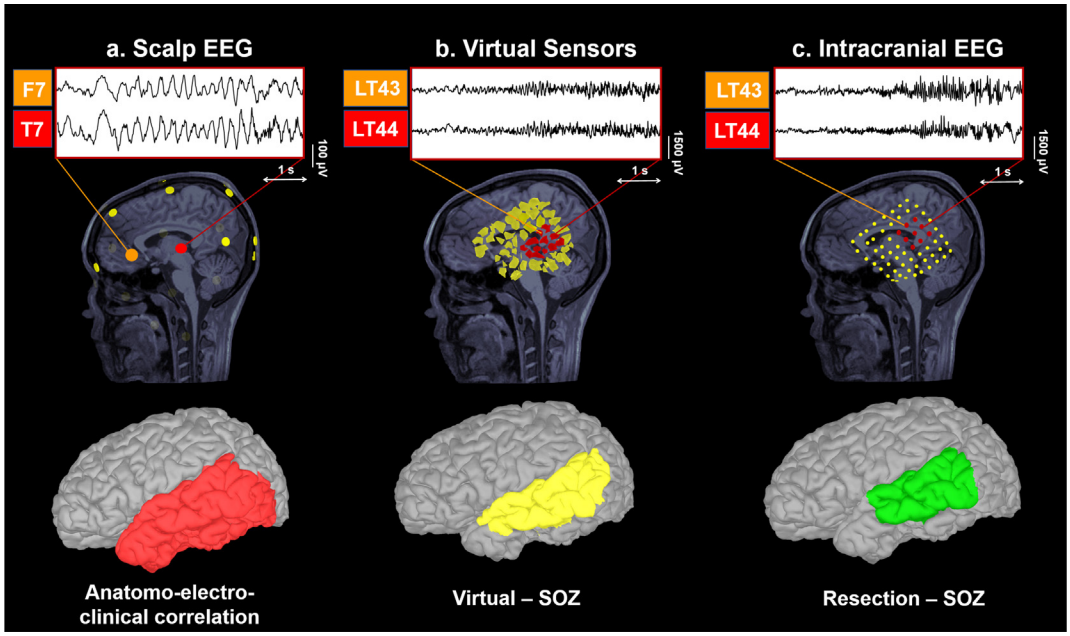

Fig. 3. Example of virtual sensors (VSs) reconstruction. VS reconstruction for patient #5. Ictal signs at seizure onset were staring with impaired awareness, repetitive vocalizations and gestural automatism with right hand. Long-term monitoring using low-density scalp EEG suggested an onset on left frontal and temporal regions. MRI showed left temporo-occipital subcortical heterotopia with associated dysmorphic hyperintense left hippocampus. VSs reconstruction at matched intracranial EEG locations pointed out to left mesial and lateral temporal regions (LT 43–44). The *virtually-defined* SOZ was anatomically concordant with the reference standard (*intracranial EEG-defined SOZ, left mesial and lateral temporal lobe*). The patient was seizure-free after surgery (Engel class IA). SOZ = Seizure Onset Zone.

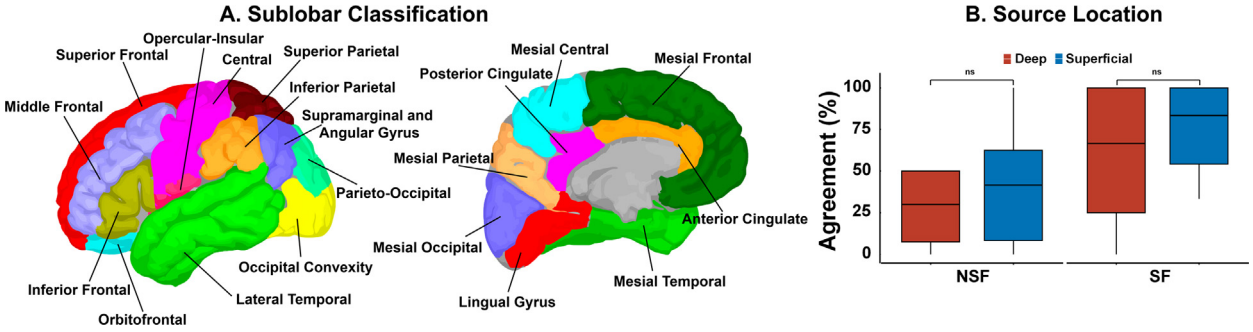

Fig. 4. Sublobar classification of cortical regions. A. Sublobar classification of cortical regions according to anatomical landmarks and brain sulci: 1. Superior Frontal; 2. Middle Frontal; 3. Inferior Frontal; 4. Orbitofrontal; 5. Lateral Temporal; 6. Occipital Convexity; 7. Parieto-Occipital region; 8. Supramarginal and Angular gyrus; 9. Inferior Parietal; 10. Superior Parietal; 11. Central region; 12. Opercular-Insular region; 13. Mesial Frontal; 14. Anterior Cingulate; 15. Mesial Temporal, including the hippocampus, the amygdala and the para-hippocampal gyrus; 16. Lingual gyrus; 17. Mesial Occipital; 18. Mesial Parietal; 19. Posterior Cingulate; 20. Mesial Central. B. Localization accuracy of the seizure-onset zone (SOZ) using virtual sensors (VSs) among patients with superficial and deep seizure onsets. Boxplot distributions of the percentage of agreement between VSs and intracranial-EEG (icEEG) defined SOZ among patients with superficial (in blue) and deep seizure onset regions (in red). We found no significant differences in the percentage of agreement based on the location of the SOZ (superficial vs deep) in both seizure-free (SF) and non-seizure-free (NSF) patients. Ns: not significant ($p > 0.05$).

concordance between the *virtually-defined SOZ* and the reference standard; and (iv) false negatives (FN), SF patients with low concordance between the *virtually-defined SOZ* and the reference standard. We assessed the following performance metrics: (i) specificity; (ii) sensitivity; (iii) accuracy; (iv) negative predictive value; and (v) positive predictive value (Ricci et al., 2021). Finally, we built non-parametric ROC curves to estimate 95% confidence intervals (CIs) for the area under the curve (AUC), sensitivity, specificity, PPV, NPV and accuracy. CIs were validated using 10,000 stratified bootstrap replicates (Carpenter and Bithell, 2000).

2.12. Statistical analysis

Patients' clinical characteristics were compared between SF and NSF patients using the χ^2 test for categorical variables and Mann-Whitney U tests for continuous variables. Shapiro-Wilk W test was used to check for normality. Wilcoxon sign-rank test was used to compare the percentage agreement of VSs and icEEG electrodes where ictal onset patterns were seen between SF and NSF patients. The measurement of agreement and 95% confidence interval (CI) between ictal electrographic patterns on VSs and the reference standard (icEEG) was determined by weighted Cohens kappa (Altman, 1991). Kappa value was interpreted according to the conventional groups: no agreement ($k < 0$); slight (0.01–0.2); fair (0.21–0.4); moderate (0.41–0.6); substantial (0.61–0.8) and almost perfect agreement (>0.8) (Landis and Koch, 1977). Fisher's exact test was used to verify the association between the concordance (above optimum cut-off) of *virtually-defined SOZ* with the reference standard and outcome. We used logistic regression to evaluate the association between the percentage agreement of the *virtually-defined SOZ* with the reference standard and the patient's outcome including other confounding variables (i.e., age, gender, duration of

epilepsy, frequency of seizures, resection volume, lesion on MRI, and temporal vs. extra-temporal/multilobar resection). Statistical analysis was performed using the R statistical package (Team, 2013). Significance level was established at $p < 0.05$. Results are reported as mean ± standard deviation or median and interquartile range for non-normally distributed data.

3. Results

3.1. Patient cohort

Thirty-five patients (21/14 males/females; mean age: 11.88 ± 5. 67 years) satisfied all inclusion and exclusion criteria. Demographic and clinical characteristics of our cohort can be found elsewhere (Ricci et al., 2021).

3.2. Ictal Patterns: Comparison between VSs and icEEG

Among ictal patterns on VSs, we found 13 patients presenting *spike-and-wave activity* (37.1%), followed by 12 patients presenting *low-voltage fast activity* (34.3%), and 10 patients presenting *rhythmic activity* $\leq$ *13 Hz* (28.6%). Among ictal patterns on icEEG, we found 14 patients presenting *rhythmic activity* $\leq$ *13 Hz* at onset (40%), followed by 11 patients presenting a *low-voltage fast activity* ictal pattern (31.4%), and 10 patients with *spike-and-wave activity* (28.6%, Fig. 5a). No differences in the ictal pattern's presentation were observed in patients presenting more than one stereotyped clinical seizure. We found moderate agreement between virtual and icEEG ictal patterns (kappa = 0.45, CI: 0.68–0.22; $p < 0.001$).

3.3. Virtually-defined SOZ: Agreement with reference standard

We observed that the *virtually-defined SOZ* was more concordant with the reference standard in SF compared to NSF patients: the percentage agreement of the VSs with the icEEG electrodes where ictal onset patterns were seen was 41.6% (2.5–50%) in NSF and 66.6% (50–100%) in SF patients ($p = 0.01$) (Fig. 5b). Logistic regression showed that the percentage agreement of VSs with the icEEG channels where ictal onset patterns were seen predicted outcome (OR: 1.03; CI: 1.01–1.06; $p = 0.04$) without interaction with other clinical confounding variables: patients with higher percentage agreement were more likely to achieve seizure freedom.

3.4. Virtually-defined SOZ: influence of SOZ location

We found that the percentage agreement between *virtually-defined SOZ* and the *icEEG-defined SOZ* did not differ among patients with superficial and deep seizure onsets: the percentage agreement was 58.3% (33.3–100%) in superficial onset regions and 50% (5–87.5%) in deeper onset regions ($p = 0.63$). Similarly, the comparison of percentage agreement between superficial and deep seizure

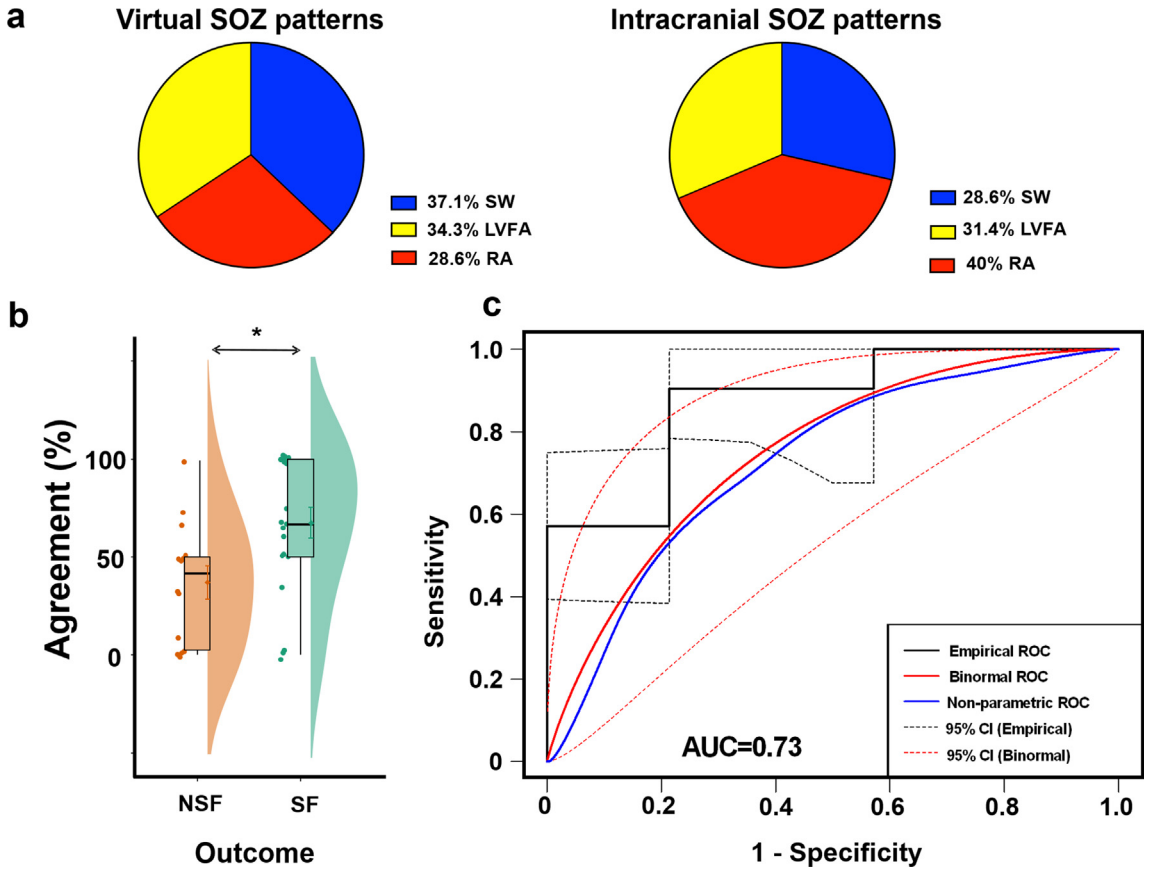

Fig. 5. Virtually-defined seizure-onset zone (SOZ) and association with clinical outcome. a. Comparison of ictal EEG patterns between virtual sensors (VSs) and intracranial EEG recordings. **b**. Raincloud plot and boxplot distribution of the percentage of agreement between intracranial EEG SOZ and *virtually-defined* SOZ (i.e., VSs showing the earliest ictal activity) and among non-seizure-free (orange) and seizure-free (green) patients. Black lines represent mean values. Circles denote mean percentage agreement for each patient. Notice how seizure-free patients present a higher percentage of agreement between *virtually-defined* SOZ and intracranial EEG SOZ electrodes ($p < 0.001$). **c**. Receiver Operating Characteristic (ROC) curve (black line) of the anatomical concordance of *virtually-defined* SOZ with intracranial EEG SOZ for the prediction of outcome (seizure-freedom). Non-parametric ROC curve (blue line), Binormal ROC curve (red line) and 95% Confidence Interval (C.I.; dotted lines) are shown. AUC = Area Under the Curve. NSF = Non seizure-free; SF = Seizure-free; SW = Spike-and-wave activity; LVFA: Low-voltage fast activity; RA: Rhythmic activity at $\leq$13 Hz.

onset regions considering only SF patients, who are proof of correct localization and resection of the EZ, failed to reveal significant differences among groups. The percentage agreement between VSs and *icEEG-defined SOZ* in SF patients was 83.3% (54.1–100%) in superficial onset regions and 66.6% (25–100%) in deeper onset regions (p = 0.42; Fig. 4B).

3.5. Prediction of surgical outcome

ROC curve analysis showed that the anatomical concordance (sublobar level) of the *virtually-defined SOZ* with the *icEEG-defined SOZ* predicted outcome (Fig. 5c) with an area under the curve (AUC) of 0.73 (95% CI, 0.57–0.89), a sensitivity of 66.7% (95% CI, 48–86%), a specificity of 78.6% (95% CI, 57.1–100%), a PPV of 83.3% (95% CI, 66.7–100%), a NPV of 61.9% (95% CI, 47.4–78.6%) and an accuracy of 71.4% (95% CI, 54.3–85.7%). Fisher exact test revealed a significant association between the anatomical concordance of the *virtually-defined SOZ* and good surgical outcome (seizure freedom, p = 0.04).

4. Discussion

Here, we propose a novel ESI-based method that identifies the SOZ and predicts the surgical outcome of children with DRE who underwent resective neurosurgery through the "implantation" of VSs that reconstructs ictal onset patterns recorded noninvasively with ldEEG. This notion derives from our main findings showing that: (i) ictal patterns estimated noninvasively with VSs present moderate agreement with those recorded invasively with icEEG; (ii) the virtually-defined SOZ is more concordance to the reference standard in SF compared to NSF patients; and (iii) delineation of the virtually-defined SOZ predicts surgical outcome. Our method might facilitate the presurgical workup and improve the planning of icEEG placement in children with DRE undergoing surgery.

4.1. Reconstructing the SOZ using virtual implantation: Comparison with icEEG

Understanding the relationship between the ictal discharges recorded noninvasively with the scalp EEG and those recorded invasively with icEEG is a challenging task. While simultaneous intracranial and scalp registrations might be proposed (Mikuni et al., 1997, Oishi et al., 2002), their clinical use is hindered by technical and practical issues including risk of infections. Here, we compared ldEEG and icEEG seizures obtained from different recording sessions. Therefore, we selected icEEG seizures that were clinically stereotyped and comparable to ldEEG. These icEEG seizures were likely involving the same epileptic foci as those recorded during ldEEG long-term monitoring. Several previous studies proposed strategies to link icEEG recording and noninvasive modalities (i.e., MEG or hdEEG) along the cortical surface to reconstruct signal at a-priori decided brain locations at the individual or group level (David et al., 2011, Grova et al., 2016, Pei et al., 2011). However, the association between icEEG recordings and EEG/MEG-reconstructed VSs was exploited to compare accuracy in terms of spikes locations (Grova et al., 2016, Murakami et al., 2016), mapping of interictal high frequency oscillations (Tamilia et al., 2021), and spectral analysis and functional networks (Juárez-Martinez et al., 2018).

Our study explored the use of ldEEG to reconstruct ictal signal on smaller regions of interest (also called VSs) that matched the icEEG implantation by using an ESI-based approach (dSPM). To our best knowledge, this is the first attempt to assess the feasibility of reconstructing ldEEG seizures using a virtual intracranial implantation. The International Federation of Clinical Neurophysiology endorses the use of hdEEG for source localization purposes (Seeck et al., 2017). This notion is supported by recent works and prospective studies that confirm the high accuracy of ESI with hdEEG in localizing the SOZ (Sohrabpour et al., 2020, Tamilia et al., 2019), and in improving the surgical outcome of patients with DRE undergoing presurgical evaluation (Duez et al., 2019, Plummer et al., 2019). However, the possibility to localize the SOZ using ESI methods and ldEEG, which is low-cost and extensively available in every epilepsy center, would offer a significant improvement in the diagnostic work-up for all those centers that lack access to sophisticated neurophysiological methods. Moreover, since the simultaneous registration of icEEG and scalp EEG recordings advocates the use of ldEEG for practical and safety purposes (Dubarry et al., 2014, Juárez-Martinez et al., 2018), our proposed methodology can be used as a pipeline for future simultaneous icEGG and scalp EEG studies.

Here, we show that this approach is feasible: the ictal onset patterns reconstructed with VSs match the icEEG recordings with a high percentage of agreement between VSs and icEEG SOZ-electrodes, especially in SF patients (median: 66.6%). The fact that the agreement between VSs and icEEG ictal patterns in our cohort fails to be higher than "moderate" (kappa = 0.45) is to some extent expected. A possible reason may derive from the findings of Pacia and Ebersole (1997) using simultaneous icEEG and surface recordings, showing that certain ictal activities, such as those restricted to the hippocampus, did not produce scalp EEG rhythms. This was explained by: (i) the small volume of the hippocampus; (ii) its curved geometry, which caused field cancellation; and (iii) the distortion effect caused by the skull and scalp tissues; with scalp EEG activity becoming evident only after propagation to adjacent temporal lobe structures. Yet, a previous study using simultaneous MEG, scalp EEG, and icEEG showed that scalp EEG signals had higher correlations with icEEG signals than MEG (Dubarry et al., 2014), although the icEEG contacts, which correlated with the scalp EEG and MEG, were different (Dubarry et al., 2014). Taken together, our own findings and previous results suggest a scenario in which the two modalities (i.e., MEG and scalp EEG) present different but complementary capacities and should best be used in combination for research and clinical purposes (Tamilia et al., 2021, Zijlmans et al., 2002).

Finally, we did not find significant differences in the localization accuracy of the SOZ using VSs between superficial and deep seizure onset regions (Fig. 4B). This notion further suggests that virtual implantation using low-density EEG may aid the localization of the SOZ at sublobar resolution, regardless of the location of the epileptogenic focus. However, it is reasonable to assume that more advanced neurophysiological techniques (i.e., hdEEG or MEG) may further improve the overall performance of virtual intracranial implantation (Cao et al., 2022, Plummer et al., 2019). Further prospective studies on large patient populations will reveal whether EEG monitoring using hdEEG or MEG will provide an added value for the localization of the SOZ using virtual implantation.

4.2. Virtual implantation using ictal ldEEG predicts surgical outcome

Previous studies showed that ESI using scalp ldEEG can offer critical information in patients evaluated for epilepsy surgery (Beniczky et al., 2013, Sharma et al., 2018, Tamilia et al., 2019, van Mierlo et al., 2017). Among other, Sharma et al., demonstrated that ictal ESI using ldEEG has high feasibility and its localization accuracy is comparable to other standard neuroimaging techniques (Sharma et al., 2018). Similarly, Foged et al. (2020), showed that ESI can provide non-redundant information in one-third of patients evaluated for epilepsy surgery. Our own findings from a recent work using standard ESI on ictal ldEEG were consistent with

such notion and showed that it has the potential to pinpoint the SOZ with an accuracy of ~30 mm (Ricci et al., 2021). However, this is not sufficient to establish the predictive value of ESI-based techniques at the individual patient level.

To answer this question, we first investigated whether VSs can localize epileptic generators, whose anatomical concordance to the reference standard may aid in assessing the patient's prognosis. We found an agreement between the *virtually-defined SOZ* with the reference standard and outcome: the higher the percentage agreement between VSs and icEEG SOZ electrodes, the better the outcome (OR: 1.03), regardless of other clinical variables. Secondly, we found that the anatomical concordance of *virtually-defined SOZ* with the reference standard allowed the prediction of seizure-freedom with a sensitivity of 66.7% (95% CI, 48–86%), a specificity of 78.6% (95% CI, 57.1–100%), and an accuracy of 71.4% (95% CI, 54.3–85.7%). This notion emphasizes the reliability of virtual implantation in guiding the placement of icEEG with high accuracy, while preserving its predictive value in terms of outcome. Our main findings are in line with the results from our previous work on ictal-ESI using ldEEG, showing an overall prognostic accuracy for surgical outcome of ESI standard methods (i.e., equivalent current dipole and standardized low-resolution magnetic tomography) of 68.5% (Ricci et al., 2021), and with those of a recent meta-analysis on ESI, which analyzed 25 ESI studies (Sharma et al., 2019). They reported an overall accuracy of ESI techniques varying from 50 and 74.84%, which is consistent with the accuracy described in our work (71.4%).

The most critical step of icEEG monitoring is the preimplantation tailoring, which should be built on a solid hypothesis derived from the combination of a detailed review of neuroimaging data and electroclinical correlations from scalp EEG recordings of seizures. Despite all the non-invasive methods actually available, icEEG electrodes may not be always implanted at optimal sites, and therefore the recorded ictal and interictal events may correspond to propagated activity from the EZ (Murakami et al., 2016, Tamilia et al., 2020, Tamilia et al., 2021). Recording from propagated activity than truly SOZ brain regions may explain the observed worse outcome in patients with lower agreement, as compared to those with clearly concordant VSs and icEEG ictal data. Thus, our results indicate that the guidance from a noninvasive and widely available modality, such as virtual implantation at target brain regions using ldEEG ictal recordings, may allow for a more comprehensive viewpoint of ictal episodes. Such additional data may provide essential information during the process of presurgical evaluation prior to the real positioning of intracranial electrodes and possibly improve epilepsy surgery outcomes.

4.3. Limitations and future directions

The first limitation of our study is its retrospective, non-randomized design since we could not directly evaluate the effect that virtual implantation had on the implantation planning of icEEG electrodes and consequently, on long-term surgical outcome. Longitudinal prospective studies with larger cohort are advocated to clarify whether virtual intracranial implantation based on ldEEG will successfully aid physicians in the surgical management of patients with DRE undergoing presurgical evaluation. A selection bias may limit the applicability of our approach: only patients referred for icEEG monitoring at our center and who had focal seizures during ldEEG monitoring were included. Although possibly biased, our sample includes patients where standard localization techniques failed to offer sufficient information for surgical planning, and thus who would benefit the most from different analytic approaches, as we suggest in our work. Yet, generalizability to patients with one-stage resection and seizures with generalized discharges or an electrodecremental pattern needs further studies. We built VSs sensors that matched the icEEG location to allow direct comparison with icEEG (the reference standard for the SOZ delineation); future studies will reveal whether a whole-brain virtual implantation may offer additive value for the delineation of the SOZ (Tamilia et al., 2021).

Finally, ldEEG and icEEG ictal events were recorded throughout different registrations. Co-registration using scalp EEG and icEEG is likely further to exploit the advantages of VSs for understanding and delineating the cortical substrates of scalp EEG recorded seizures (Tao et al., 2007).

4.4. Conclusion

We revealed the feasibility of a noninvasive delineation of the SOZ using virtual intracranial implantation and seizures recorded with ldEEG in children with DRE and showed its prognostic value for surgical outcome. Our results suggest that by using VSs at the anatomical location of the planned icEEG, it is possible to obtain valuable information, thus offering a potential useful clinical tool in the pre-surgical evaluation of children with complex DRE. These results open up the possibility of using ldEEG seizures to "foresee" later icEEG findings at various brain locations and use this information during the icEEG electrodes implantation's decision. This non-invasive localization of the SOZ may augment icEEG and surgical planning and offer a boost in the presurgical workup of children with DRE, potentially improving outcomes of epilepsy surgery.

Declaration of Competing Interest

The authors declare that they have no known competing financial interests or personal relationships that could have appeared to influence the work reported in this paper.

Acknowledgments

This study was supported by the National Institute of Neurological Disorders & Stroke (RO1NS104116-01A1, PI: C. Papadelis; and R21NS101373-01A1, PIs: C. Papadelis and S. Stufflebeam). The findings of this study were presented at the pediatric highlights of the 2021 Annual Meeting of the American Epilepsy Society. The authors acknowledge that the cohort of patients evaluated in this study (35 patients) was also employed in a previous work from our group (Ricci et al., 2021).

Ethical publication statement

All the authors confirm that they have read the Journal's position on issues involved in ethical publication and affirm that this report is consistent with those guidelines.

References

Agirre-Arrizubieta Z, Huiskamp GJM, Ferrier CH, van Huffelen AC, Leijten FSS. Interictal magnetoencephalography and the irritative zone in the electrocorticogram. Brain 2009;132(11):3060–71.

Alhilani M, Tamilia E, Ricci L, Ricci L, Grant PE, Madsen JR, et al. Ictal and interictal source imaging on intracranial EEG predicts epilepsy surgery outcome in children with focal cortical dysplasia. Clin Neurophysiol 2020;131(3):734–43.

Altman DG. Practical statistics for medical research. London and New York: Chapman and Hall; 1991.

Beniczky S, Lantz G, Rosenzweig I, Åkeson P, Pedersen B, Pinborg LH, et al. Source localization of rhythmic ictal EEG activity: a study of diagnostic accuracy following STARD criteria. Epilepsia 2013;54(10):1743–52.

Cao M, Galvis D, Vogrin SJ, Woods WP, Vogrin S, Wang F, et al. Virtual intracranial EEG signals reconstructed from MEG with potential for epilepsy surgery. Nat Commun 2022;13(1). https://doi.org/10.1038/s41467-022-28640-x.

Carpenter J, Bithell J. Bootstrap confidence intervals: when, which, what? A practical guide for medical statisticians. Stat Med 2000;19(9):1141–64.

Chu CJ. High density EEG-What do we have to lose? Clin Neurophysiol 2015;126(3):433–4.

Cossu M, Cardinale F, Castana L, Citterio A, Francione S, Tassi L, et al. Stereoelectroencephalography in the presurgical evaluation of focal epilepsy: a retrospective analysis of 215 procedures. Neurosurgery 2005;57(4):706–18.
Dale AM, Fischl B, Sereno MI. Cortical surface-based analysis: I. Segmentation and surface reconstruction. Neuroimage 1999;9(2):179–94.
Dale AM, Liu AK, Fischl BR, Buckner RL, Belliveau JW, Lewine JD, et al. Dynamic statistical parametric mapping: combining fMRI and MEG for high-resolution imaging of cortical activity. Neuron 2000;26(1):55–67.
David O, Blauwblomme T, Job A-S, Chabardès S, Hoffmann D, Minotti L, et al. Imaging the seizure onset zone with stereo-electroencephalography. Brain 2011;134(10):2898–911.
Di Giacomo R, Uribe-San-Martin R, Mai R, Francione S, Nobili L, Sartori I, et al. Stereo-EEG ictal/interictal patterns and underlying pathologies. Seizure 2019;72:54–60.
Dubarry A-S, Badier J-M, Trébuchon-Da Fonseca A, Gavaret M, Carron R, Bartolomei F, et al. Simultaneous recording of MEG, EEG and intracerebral EEG during visual stimulation: from feasibility to single-trial analysis. Neuroimage 2014;99:548–58.
Duez L, Tankisi H, Hansen PO, Sidenius P, Sabers A, Pinborg LH, et al. Electromagnetic source imaging in presurgical workup of patients with epilepsy: A prospective study. Neurology 2019;92(6):e576–86.
Engel Jr J, Van Ness PC, Rasmussen TB, Ojemann LM. Outcome with respect to epileptic seizures. In: Engel J, editor. Surgical treatment of the epilepsies. 2nd ed. New York: Raven Press; 1993. p. 609–21.
Foged MT, Martens T, Pinborg LH, Hamrouni N, Litman M, Rubboli G, et al. Diagnostic added value of electrical source imaging in presurgical evaluation of patients with epilepsy: A prospective study. Clin Neurophysiol 2020;131(1):324–9.
Gramfort A, Papadopoulo T, Olivi E, Clerc M. OpenMEEG: opensource software for quasistatic bioelectromagnetics. Biomed Eng Online 2010;9(1):45. https://doi.org/10.1186/1475-925X-9-45.
Grova C, Aiguabella M, Zelmann R, Lina J-M, Hall JA, Kobayashi E. Intracranial EEG potentials estimated from MEG sources: A new approach to correlate MEG and iEEG data in epilepsy. Hum Brain Mapp 2016;37(5):1661–83.
Hillebrand A, Singh KD, Holliday IE, Furlong PL, Barnes GR. A new approach to neuroimaging with magnetoencephalography. Hum Brain Mapp 2005;25(2):199–211.
Juárez-Martinez EL, Nissen IA, Idema S, Velis DN, Hillebrand A, Stam CJ, et al. Virtual localization of the seizure onset zone: Using non-invasive MEG virtual electrodes at stereo-EEG electrode locations in refractory epilepsy patients. Neuroimage Clin 2018;19:758–66.
Landis JR, Koch GG. The measurement of observer agreement for categorical data. Biometrics 1977;33(1):159. https://doi.org/10.2307/2529310.
Lüders HO, Najm I, Nair D, Widdess-Walsh P, Bingman W. The epileptogenic zone: general principles. Epileptic Disord 2006;8(2):1–9.
Mikuni N, Nagamine T, Ikeda A, Terada K, Taki W, Kimura J, et al. Simultaneous recording of epileptiform discharges by MEG and subdural electrodes in temporal lobe epilepsy. Neuroimage 1997;5(4):298–306.
Mohamed IS, Otsubo H, Ferrari P, Sharma R, Ochi A, Elliott I, et al. Source localization of interictal spike-locked neuromagnetic oscillations in pediatric neocortical epilepsy. Clin Neurophysiol 2013;124(8):1517–27.
Mullin JP, Shriver M, Alomar S, Najm I, Bulacio J, Chauvel P, et al. Is SEEG safe? A systematic review and meta-analysis of stereo-electroencephalography–related complications. Epilepsia 2016;57(3):386–401.
Murakami H, Wang ZI, Marashly A, Krishnan B, Prayson RA, Kakisaka Y, et al. Correlating magnetoencephalography to stereo-electroencephalography in patients undergoing epilepsy surgery. Brain 2016;139(11):2935-47.
Nemtsas P, Birot G, Pittau F, Michel CM, Schaller K, Vulliemoz S, et al. Source localization of ictal epileptic activity based on high-density scalp EEG data. Epilepsia 2017;58(6):1027–36.
Nissen IA, Stam CJ, Reijneveld JC, van Straaten IECW, Hendriks EJ, Baayen JC, et al. Identifying the epileptogenic zone in interictal resting-state MEG source-space networks. Epilepsia 2017;58(1):137–48.
Oishi M, Otsubo H, Kameyama S, Morota N, Masuda H, Kitayama M, et al. Epileptic spikes: magnetoencephalography versus simultaneous electrocorticography. Epilepsia 2002;43(11):1390–5.
Pacia SV, Ebersole JS. Intracranial EEG substrates of scalp ictal patterns from temporal lobe foci. Epilepsia 1997;38(6):642–54.
Pei X, Leuthardt EC, Gaona CM, Brunner P, Wolpaw JR, Schalk G. Spatiotemporal dynamics of electrocorticographic high gamma activity during overt and covert word repetition. Neuroimage 2011;54(4):2960–72.
Pellegrino G, Hedrich T, Chowdhury R, Hall JA, Lina J-M, Dubeau F, et al. Source localization of the seizure onset zone from ictal EEG/MEG data. Hum Brain Mapp 2016;37(7):2528–46.
Perucca P, Dubeau F, Gotman J. Intracranial electroencephalographic seizure-onset patterns: effect of underlying pathology. Brain 2013;137(1):183–96.
Plummer C, Vogrin SJ, Woods WP, Murphy MA, Cook MJ, Liley DTJ. Interictal and ictal source localization for epilepsy surgery using high-density EEG with MEG: a prospective long-term study. Brain 2019;142(4):932–51.
Ricci L, Tamilia E, Alhilani M, Alter A, Scott Perry , Madsen JR, et al. Source imaging of seizure onset predicts surgical outcome in pediatric epilepsy. Clin Neurophysiol 2021;132(7):1622–35.
Rosenow F, Lüders H. Presurgical evaluation of epilepsy. Brain 2001;124(9):1683–700.
Russo A, Jayakar P, Lallas M, Miller I, Hyslop A, Korman B, et al. The diagnostic utility of 3D electroencephalography source imaging in pediatric epilepsy surgery. Epilepsia 2016;57(1):24–31.
Ryvlin P, Cross JH, Rheims S. Epilepsy surgery in children and adults. Lancet Neurol 2014;13(11):1114–26.
Seeck M, Koessler L, Bast T, Leijten F, Michel C, Baumgartner C, et al. The standardized EEG electrode array of the IFCN. Clin Neurophysiol 2017;128(10):2070–7.
Sharma P, Scherg M, Pinborg LH, Fabricius M, Rubboli G, Pedersen B, et al. Ictal and interictal electric source imaging in pre-surgical evaluation: a prospective study. Eur J Neurol 2018;25(9):1154–60.
Sharma P, Seeck M, Beniczky S. Accuracy of interictal and ictal electric and magnetic source imaging: a systematic review and meta-analysis. Front Neurol 2019;10. https://doi.org/10.3389/fneur.2019.0125010.3389/fneur.2019.01250.s00110.3389/fneur.2019.01250.s00210.3389/fneur.2019.01250.s003.
Sohrabpour A, Cai Z, Ye S, Brinkmann B, Worrell G, He B. Noninvasive electromagnetic source imaging of spatiotemporally distributed epileptogenic brain sources. Nat Commun 2020;11(1):1–15.
Song J, Davey C, Poulsen C, Luu P, Turovets S, Anderson E, et al. EEG source localization: sensor density and head surface coverage. J Neurosci Methods 2015;256:9–21.
Staljanssens W, Strobbe G, Van Holen R, Keereman V, Gadeyne S, Carrette E, et al. EEG source connectivity to localize the seizure onset zone in patients with drug resistant epilepsy. Neuroimage Clin 2017;16:689–98.
Tadel F, Baillet S, Mosher JC, Pantazis D, Leahy RM. Brainstorm: a user-friendly application for MEG/EEG analysis. Comput Intell Neurosci 2011;2011:1–13.
Tamilia E, AlHilani M, Tanaka N, Tsuboyama M, Peters JM, Grant PE, et al. Assessing the localization accuracy and clinical utility of electric and magnetic source imaging in children with epilepsy. Clin Neurophysiol 2019;130(4):491–504.
Tamilia E, Dirodi M, Alhilani M, Grant PE, Madsen JR, Stufflebeam SM, et al. Scalp ripples as prognostic biomarkers of epileptogenicity in pediatric surgery. Ann Clin Transl Neurol 2020;7(3):329–42.
Tamilia E, Matarrese MAG, Ntolkeras G, Grant PE, Madsen JR, Stufflebeam SM, et al. Noninvasive Mapping of Ripple Onset Predicts Outcome in Epilepsy Surgery. Ann Neurol 2021;89(5):911–25.
Tao JX, Baldwin M, Hawes-Ebersole S, Ebersole JS. Cortical Substrates of Scalp EEG Epileptiform Discharges. J Clin Neurophysiol 2007;24(2):96–100.
Team RC. R: A language and environment for statistical computing; 2013.
van Mierlo P, Strobbe G, Keereman V, Birot G, Gadeyne S, Gschwind M, et al. Automated long-term EEG analysis to localize the epileptogenic zone. Epilepsia Open 2017;2(3):322–33.
Verma A, Radtke R. EEG of partial seizures. J Clin Neurophysiol 2006;23(4):333–9.
Zijlmans M, Huiskamp GM, Leijten FSS, van der Meij WM, Wieneke G, van Huffelen AC. Modality-specific spike identification in simultaneous magnetoencephalography/electroencephalography: a methodological approach. J Clin Neurophysiol 2002;19(3):183–91.